Applied Physics A (2019) 125:207
https://doi.org/10.1007/s00339-019-2479-y

Applied Physics A
Materials Science & Processing

Synthesis and properties of $BaWO_4$ nanocrystals prepared using a reverse microemulsion method

Guojun Zha[1,2] · Naigen Hu[2] · Minhua Jiang[1,2] · Xiangming Zeng[2] · Haoqing Hou[1]

Received: 6 December 2018 / Accepted: 6 February 2019 / Published online: 23 February 2019
© Springer-Verlag GmbH Germany, part of Springer Nature 2019

Abstract
Barium tungstate ($BaWO_4$) nanocrystals were successfully synthesized using a reverse microemulsion method. The effects of the molar ratio of water to surfactant (ω_o), reactant concentration, and aging time on the size and morphology of the $BaWO_4$ nanocrystals were investigated. The obtained products were characterized by scanning electron microscopy and X-ray diffraction (XRD). The experimental results showed that the morphology and size of the as-prepared $BaWO_4$ nanocrystals were greatly affected by the ω_o and the initial concentration, but no obvious effect by the aging time. XRD analysis showed that the $BaWO_4$ nanocrystals synthesized had the high purity under conditions of initial reactant concentration of 0.2 mol/L, ω_o of 40, at temperature of 50 °C and aging time of 24 h. Photoluminescent spectra revealed that $BaWO_4$ crystallites displayed a very strong peak at 351 nm under different aging time.

1 Introduction

Recently, micro- and nanoluminescent materials have attracted wide attention and interest, $BaWO_4$ nanomaterials with a white tungsten appearance has interesting properties such as photoluminescence, thermoluminescence and stimulated Raman scattering, and show potential application in fields such as optoelectronics, medicine, and spectroscopy [1–3], especially as fluorescent material, it has good application potential in optical field [4–6]. Various $BaWO_4$ nanomaterials with different morphologies have been prepared using a range of methods, such as reverse micelle [4], solution route [5, 6], template-free precipitation [7], chemical bath deposition [8], co-precipitation [9–11], hydrothermal [12, 13], and template techniques [14, 15]. These methods usually require high temperature or complex equipment, and relatively long reaction time, which hinders the application of $BaWO_4$ to some extent.

As an important method for the synthesis of nanomaterials, microemulsion method has been widely used for the synthesis of $BaWO_4$ nanomaterials. The microemulsion could be classified to two kinds: positive-phase (O/W) and reverse-phase (W/O) microemulsion. He et al. [3] reported the synthesis of $BaWO_4$ nanocrystals with hedgehog-shaped, bundle-like, and rod-like scheelite structures using a positive-phase microemulsion method through controlling the concentration of surfactants. The reverse-phase microemulsion method can be widely used as a microreactor for the purpose of controlling the size and shape of particles conveniently through controlling ω_o (ω_o is the molar ratio of water to surfactant), reactant concentration [16, 17]. Zhang et al. [17] reported fishbone-like nanoassembled $BaWO_4$ structures which could be prepared using a reverse-phase microemulsion method. However, there is no study on the effect of ω_o, reactant concentration, and aging time on the size and morphology of the $BaWO_4$ nanocrystals. In this study, we report the synthesis of $BaWO_4$ nanocrystals by reverse microemulsion method. The effects of ω_o, reactant concentration, and aging time on the size and morphology of the $BaWO_4$ nanocrystals were investigated and high optical quality was confirmed by testing them in photoluminescent spectra.

✉ Guojun Zha
zhaguojun_8@163.com

[1] College of Chemistry and Chemical Engineering, Jiangxi Normal University, Nanchang, China

[2] School of New Energy Science and Engineering, Xinyu University, Xinyu, China

2 Experimental

2.1 Preparation of inverse microemulsion A

Preparation of Na_2WO_4 reverse microemulsion A: 25 mL cyclohexane, 6.78 mL surfactants (Triton X-100), and 2 mL 0.2 mol/L Na_2WO_4 solution were added to a round-bottom flask sequentially under continuously magnetic stirring (500 rpm). Then, 2.78 mL cosurfactant (1-hexanol) was added to the mixture and was stirred for 15 min via strong magnetic stirring (1000 rpm), until a transparent and reverse microemulsion was obtained. In that case, the molar ratio of water to surfactant (ω_o) is 10, and the molar ratio of cosurfactant to surfactant (P) was calculated, which is the optimal value, it is 2.01, the inverse microemulsion A with ω_o value of 20, 30, 40, and 50 was prepared under the same conditions (Table 1).

Preparation of $Ba(NO_3)_2$ reverse microemulsion B: the Na_2WO_4 solution was changed to $Ba(NO_3)_2$ solution, and the reverse microemulsion B was prepared using the same methodology as that of the microemulsion A.

2.2 Preparation of $BaWO_4$

$BaWO_4$ nanocrystals were prepared using a reverse microemulsion route, as shown in Fig. 1. The $Ba(NO_3)_2$ reverse microemulsion B was slowly mixed with the Na_2WO_4 reverse microemulsion A and gentle magnetically agitated for 1 h to let the system white and turbid.

Then, the mixture reverse microemulsion was aged at 50 °C for 24 h and a white precipitate was obtained. After separating the white precipitate by centrifugation and removing the adsorbed surface-active agent and other organic solvents by ultrasonically washing for five times using absolute ethanol, the $BaWO_4$ product was obtained.

2.3 Characterization of the nanocrystals BaWO4

To avoid conglomeration and aggregation, the $BaWO_4$ nanocrystals were dispersed in an anhydrous ethanol under the assistance of ultrasonic for 15 min. Then, a small amount of the dispersion was dropped on to a conductive glass slide and dried in a drying oven for 1 h to prepare samples for characterization. These samples were characterized using scanning electron microscopy (SEM; JEOL JSM-6300) and X-ray diffraction (XRD; D8 ADVANCE X'pertPro diffractometer). The room-temperature photoluminescent (PL; perkin-elmer LS55) spectra of the samples were obtained on a fluorescence spectrometer.

Table 1 Calculate the amount of surfactants and cosurfactant based on $P = 2.01$

ω_0	$V_{cyclohexane}$ (mL)	$V_{surfactants}$ (mL)	$V_{cosurfactant}$ (mL)	$V_{sodium\ tungstate\ or\ barium\ nitrate\ solution}$ (mL)
10	25	6.78	2.78	2
20	25	3.39	1.38	2
30	25	2.26	0.93	2
40	25	1.70	0.70	2
50	25	1.36	0.56	2

Characterization of the nanocrystals $BaWO_4$

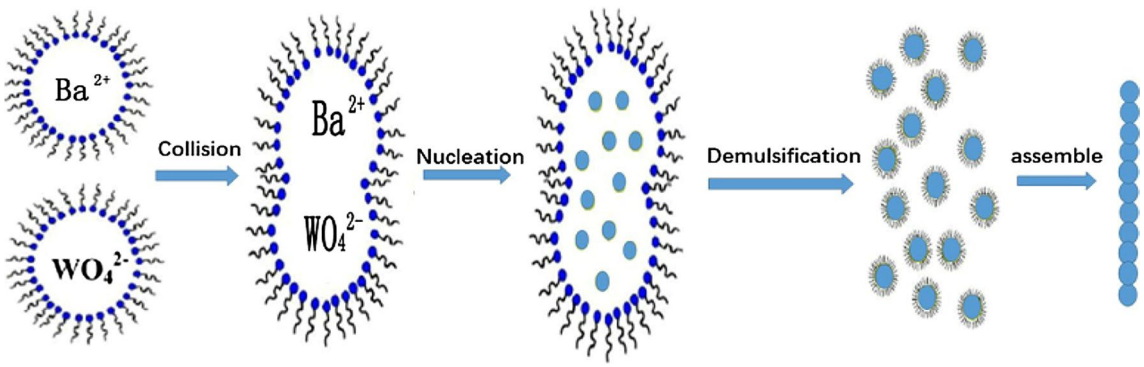

Fig. 1 Schematic diagram of $BaWO_4$ nanocrystals using a reverse microemulsion route

3 Results and discussion

Figure 2 shows that the length and diameter of the obtained $BaWO_4$ nanocrystals varied with ω_o under a concentration of $Ba(NO_3)_2$ solution of 0.2 mol/L, a temperature of 50 °C, and an aging time of 24 h. The length of the $BaWO_4$ nanocrystals varies approximately, such as 250 nm in Fig. 2a, 750 nm in Fig. 2b, 3100 nm in Fig. 2c, and 4200 nm in Fig. 2d. The diameters of the $BaWO_4$ nanocrystals increased with ω_o, which are approximately 20, 70, 260, and 420 nm with ω_o of 20, 30, 40, and 50, respectively.

With the increase of ω_o, the amount of water is 2 ml and the amount of surfactants is relatively insufficient, so the water core is prone to deformation and changes from a regular spherical shape to a rod shape. When the microemulsion (A) and the microemulsion (B) were mixed and stirred, the water nuclei of the rod-shaped reverse micelles in the microemulsion collided with each other, which leads to the fusion and self-assembly of two water nuclei into a rod-shaped water nucleus containing Ba^{2+} and WO_4^{2-}, and $BaWO_4$ is nucleated and grown in this water nucleus, forming several nanoparticles, which are restricted by the template of the rod-shaped water nucleus, and, thus, are clustered and arranged into the rod-shaped morphology [18, 19].

Figure 2 also shows that the morphology of $BaWO_4$ nanocrystals with ω_o of 40 is the best, the morphology is the most regular, the rod size and the length are uniform, but ω_o is 50, the shape of some rods becomes irregular or massive, both the rod size and the length are uneven, indicating that the water core has been deformed. The experimental results show that, when ω_o is 60, the product is no longer available, indicating that ω_o of 50 is in a transition state that cannot form a water–nucleus interface membrane well.

Figure 3 shows that the average length of the $BaWO_4$ nanocrystals is 2100 nm in Fig. 3a, 2900 nm in Fig. 3b, 3200 nm in Fig. 3c, and the average diameters are 120, 210, and 280 nm, respectively, when $\omega_o = 40$, the aging

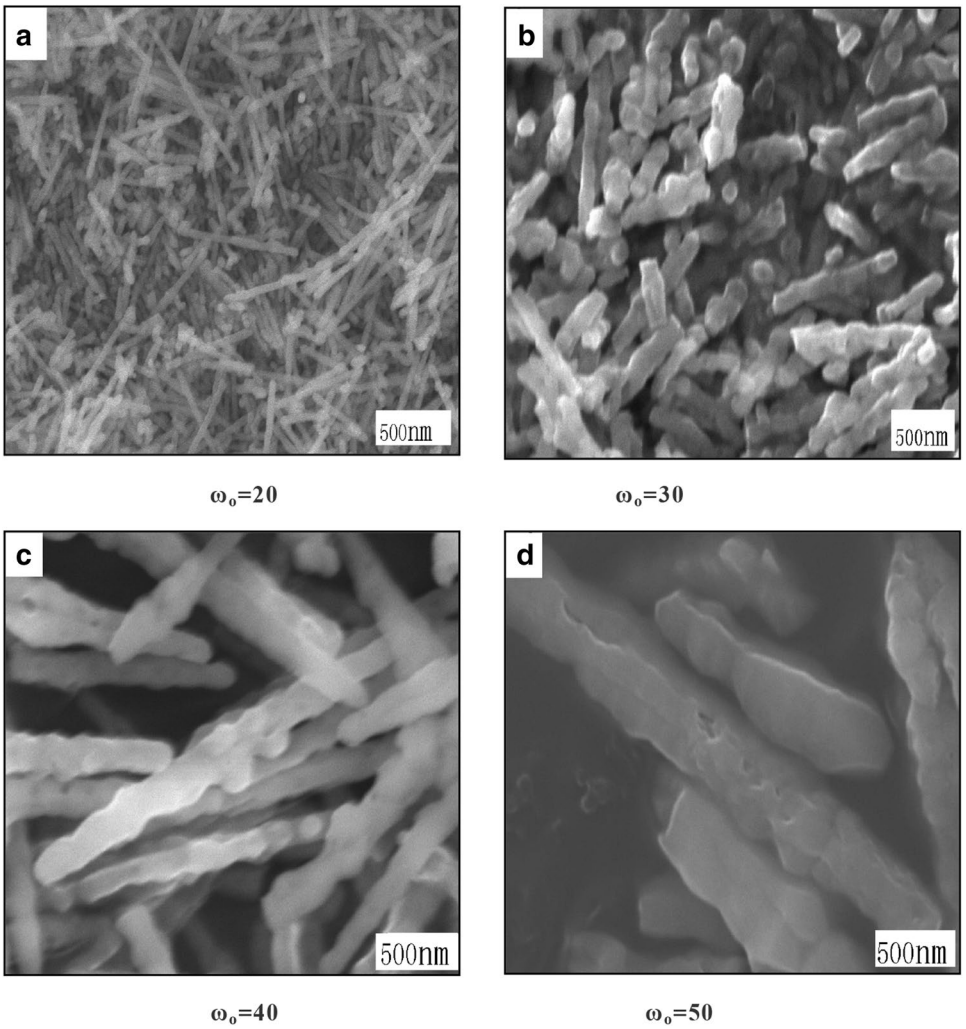

Fig. 2 SEM morphology of $BaWO_4$ under different ω_o values

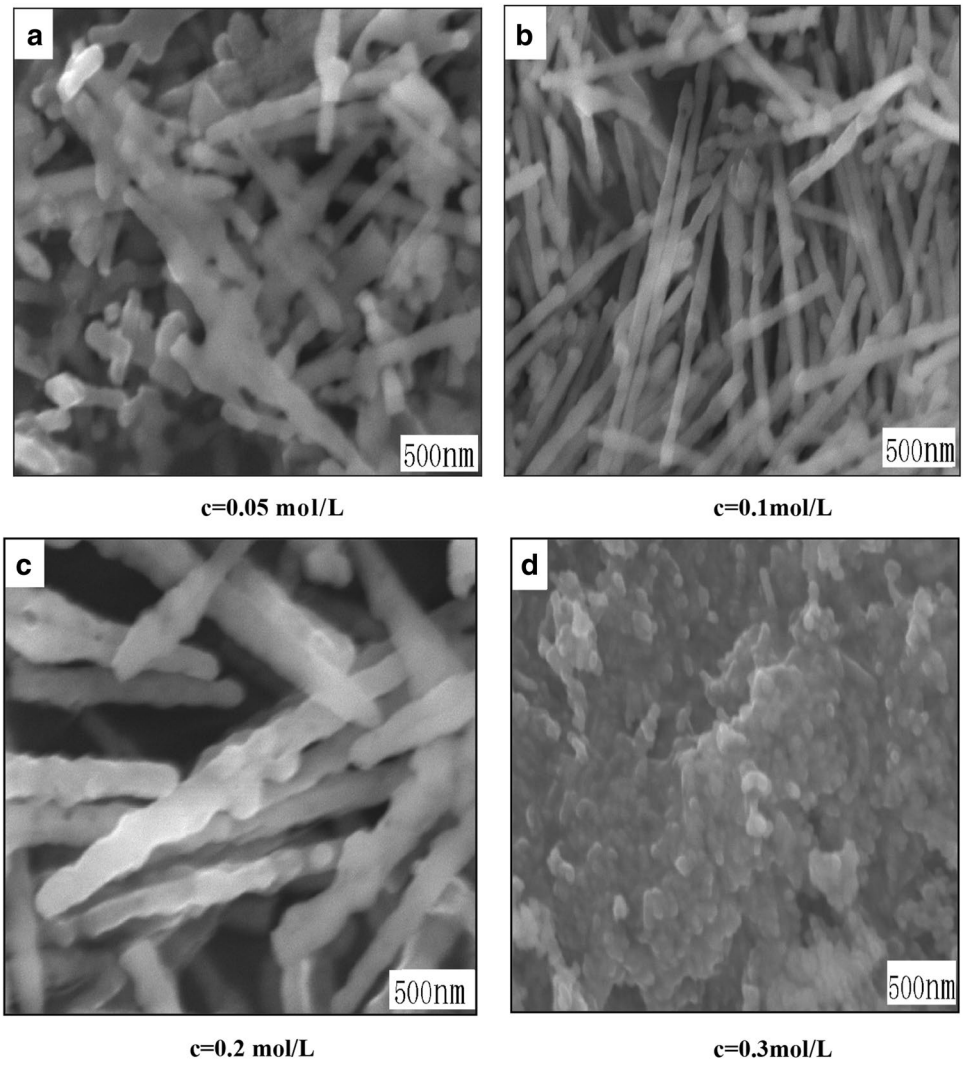

Fig. 3 SEM morphology of $BaWO_4$ under different initial concentrations

time is 24 h, the temperature is 50 °C, and the $Ba(NO_3)_2$ concentrations are 0.05, 0.1, 0.20, and 0.3 mol/L, respectively. The length and diameter of the $BaWO_4$ nanocrystals increase with the concentration of the $Ba(NO_3)_2$ solution, it is because the amount of reactant contained in water core increases with the concentration of the $Ba(NO_3)_2$ solution. Thus, this leads to the increase of the length and diameter of $BaWO_4$ nanocrystals.

In addition, Fig. 3d shows that when the concentration of $Ba(NO_3)_2$ solution reaches 0.30 mol/L, the prepared microemulsion system becomes turbid and cannot form a uniform and stable microemulsion system, resulting in the formation of the $BaWO_4$ agglomeration phenomenon. This is due to the concentration of the solution being higher and with more charges present, and thus, the particles become extremely unstable and form agglomeration.

Figure 4 shows the SEM photographs of $BaWO_4$ nanocrystals under $Ba(NO_3)_2$ concentration which is 0.2 mol/L, $t = 50$ °C, $\omega_o = 40$, and aging time of 24, 48, and 72 h, respectively. The average length of the $BaWO_4$ nanocrystals is about 4100 nm in Fig. 4a, 4200 nm in Fig. 4b, and 4000 nm in Fig. 4c, respectively, the average diameters are about 220, 240, and 230 nm, in turn, illustrating that aging time has no obvious effect on the length and the diameters of the $BaWO_4$ nanocrystals, this is because crystallization and dissolution form a balance.

Figure 4 also shows that photographs of $BaWO_4$ nanocrystals are rod shape, it is because that Triton X-100 is a non-ionic surfactant and its micelles have a little effect on the confinement of $BaWO_4$ nanocrystals. When $Ba(NO_3)_2$ and Na_2WO_4 aqueous droplets are added to the Triton X-100 solution, Ba^{2+} and WO_4^{2-} are ionized, respectively, and then, the concentration products of $Ba(NO_3)_2$ and Na_2WO_4 reach the concentration product constant of $BaWO_4$, which form fine $BaWO_4$ nuclei and the solution becomes supersaturated. During the subsequent crystal growth process, larger particles swallow smaller particles to grow the $BaWO_4$ nanocrystals [20].

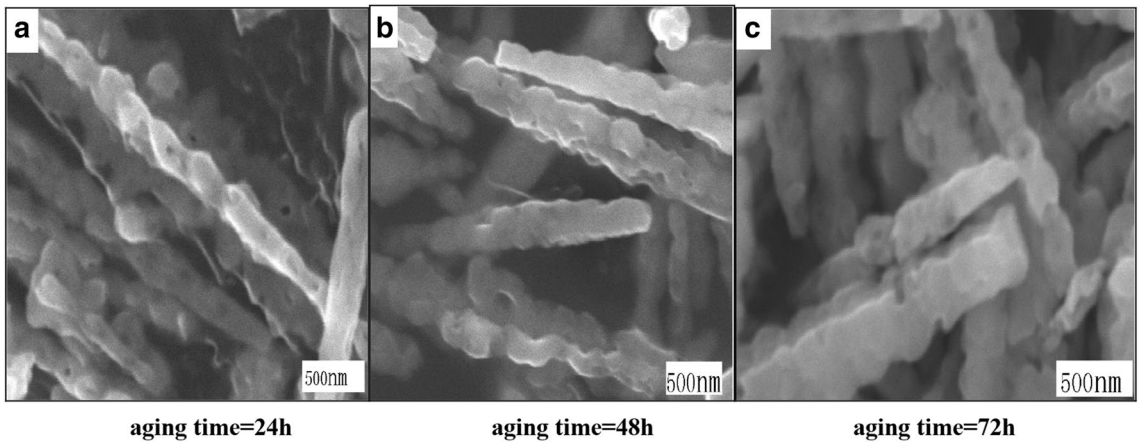

Fig. 4 SEM morphology of $BaWO_4$ under different aging time

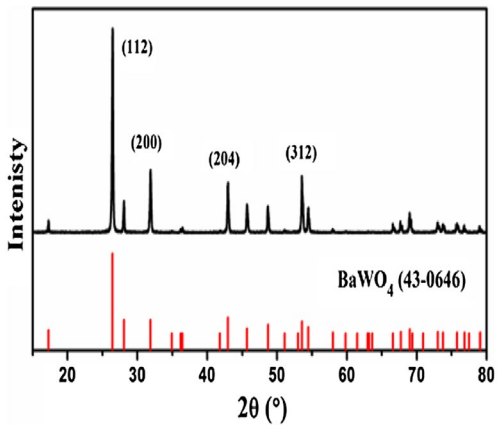

Fig. 5 XRD spectra of $BaWO_4$

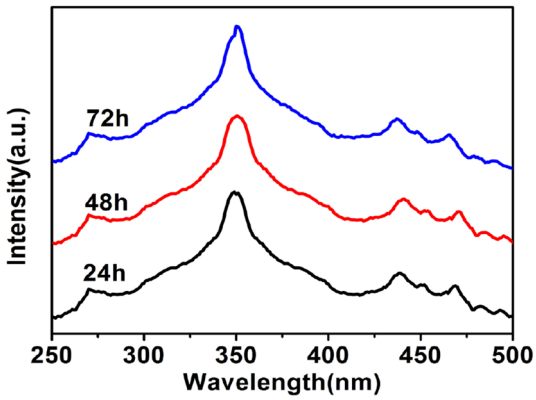

Fig. 6 PL spectrum of $BaWO_4$ under different aging time

Figure 5 shows the XRD spectra of $BaWO_4$ nanocrystals synthesized by hydrothermal reaction at 50 °C during an aging time of 24 h, $Ba(NO_3)_2$ concentration of 0.2 mol/L, and $\omega_o = 40$ under the action of surfactant Triton X-100. It can be calculated by the lattice parameters $a = b = 0.5610$ nm and $c = 1.2681$ nm and observed that the main diffraction peaks of the sample are consistent with the standard cards of tetragonal $BaWO_4$ (JCPDS, NO. 43–0646, $a = b = 0.5612$ nm and $c = 1.2706$ nm), which indicates that the synthesized $BaWO_4$ nanocrystals have good high crystallinity. No other impurity peaks can be observed in Fig. 5, indicating that the products were pure tetragonal $BaWO_4$ nanocrystals.

PL properties of the as-prepared $BaWO_4$ samples at different aging time (24, 48, and 72 h) were also investigated. As shown in Fig. 6, three samples show emission peaks at 351 nm, which have a certain blue shift compared with references [17, 19], indicating that the fluorescence properties of nanomaterials are greatly affected by their size and morphology. However, besides the dominant peak at 351 nm, some weak peaks at the positions around 440 nm, 465 nm, and 275 nm; it is because that the fluorescence emission of $BaWO_4$ powder was caused by its structural defects [21]. Furthermore, PL spectra of three samples have no obvious difference with an aging time, illustrating that aging time has no obvious effect on the length and the diameters of the $BaWO_4$ nanocrystals.

4 Conclusions

$BaWO_4$ nanocrystals were synthesized using a reverse microemulsion method and is provided with an easy way to operate. The particle size and shape of the $BaWO_4$ nanocrystals increased with ω_o. The length of the $BaWO_4$ nanocrystals ranged from 250 to 4200 nm and the diameter from 20 to 420 nm. The initial concentration of the reactants greatly influenced the morphology of the materials. The length of the $BaWO_4$ nanocrystals ranged from 2100 to 3200 nm, and the diameters ranged from 120 to 280 nm. The aging time

was found to have no obvious effect on the size and shape of the particles, and the crystallinity of the $BaWO_4$ crystals synthesized was found to be high under conditions of a 50 °C temperature, an aging time of 24 h, $Ba(NO_3)_2$ concentration of 0.2 mol/L, and a ω_o value of 40. It exhibits an excellent PL property and that their emission peak locates at 351 nm.

Acknowledgements This work was supported by the Natural Science Foundation of China (51664047) and the Foundations from the Department of Education in Jiangxi Province (GJJ161187, JY1577, and GJJ151209).

References

1. L.I. Ivleva, I.S. Voronina, P.A. Lykov et al., Growth of optically homogeneous $BaWO_4$ single crystals for Raman lasers. J Cryst. Growth **304**(1), 108 (2007)
2. M. Tyagi, S.C. Sabharwal et al., Luminescence properties of $BaWO_4$ single crystal. J. Lumin. **128**(9), 1528 (2008)
3. J.H. He, M. Han, X.P. Shen, Crystal hierarchically splitting in growth of $BaWO_4$ in positive cat-anionic microemulsion. J Cryst. Growth **310**(21), 4581 (2008)
4. H.T. Shi, L.M. Qi, J.M. Ma et al., Polymer-directed synthesis of penniform $BaWO_4$ nanostructures in reverse Micelles. J. Am. Chem. Soc. **125**(3), 450 (2003)
5. Y. Shen, W. Li, T. Li, Microwave-assisted synthesis of $BaWO_4$ nanoparticles and its photoluminescence properties. Mater. Lett. **65**, 2956 (2011)
6. Y.K. Yin, Z.B. Gan, Y.Z. Sun et al., Controlled synthesis and photoluminescence properties of $BaXO_4$ (X = W, Mo) hierarchical nanostructures via a facile solution route. Mater. Lett. **64**, 789 (2010)
7. X.M. Wang, H.Y. Xu, H. Wang et al., Morphology-controlled $BaWO_4$ powders via a template—free precipitation technique. J. Cryst. Growth **28**(41), 254 (2005)
8. R. Wang, C. Liu, J. Zeng et al., Fabrication and morphology control of $BaWO_4$ thin films by microwave assisted chemical bath deposition. J Solid State Chem. **182**, 677 (2009)
9. F.M. Pontes, M.A.M.A. Maurera, A.G. Souza et al., structural and optical characterization of $BaWO_4$ and $PbWO_4$ thin films prepared by a chemical route. J.Eur. Ceram. Soc **2**, 3001 (2003)
10. M.C. Oliveira, L. Gracia, I.C. Nogueira et al., Synthesis and morphological transformation of $BaWO_4$ crystals: experimental and theoretical insights. Ceram. Int. **42**(9), 10913 (2016)
11. L.S. Cavalcante, F.M.C. Batista, M.A.P. Almeida et al., Structural refinement, growth process, photoluminescence and photocatalytic properties of $(Ba_{1-x}Pr_{2x/3})WO_4$ crystals synthesized by the coprecipitation method. RSC Adv. **2**, 6438 (2012)
12. G. Jia, D.B. Dong, C. Song et al., Synthesis, formation process, and luminescence properties of monodisperse barium tungstate hierarchical ellipsoidal particles. Sci. Adv. Mater. **6**(4), 808 (2014)
13. B. Sun, Y. Liu, W. Zhao, J. Wu et al., Hydrothermal preparation and whitelight-controlled resistive switching behavior of $BaWO_4$ nanospheres. NanoMicro Lett. **7**, 80 (2015)
14. Z.J. Luo, H.M. Li, J.X. Xia et al., Microwave-assisted synthesis of barium tungstate nanosheets and nanobelts by using polymer PVP micelle as templates. Mater. Lett. **61**(8–9), 1845 (2007)
15. J.K. Liu, Q.S. Wu, Y.P. Ding, Controlled synthesis of different morphologies of $BaWO_4$ crystals through biomembrane/organic-addition supramolecule templates. Cryst. Growth Des. **5**(2), 445 (2005)
16. L.P. Chen, Y.H. Gao, J.L. Zhu, Luminescent properties of $BaWO_4$ films prepared by cell electrochemical technique. Mater. Lett. **62**, 3434 (2008)
17. X. Zhang, Y. Xie, F. Xu et al., Growth of $BaWO_4$ fishbone like Nanostructures in w/o microemulsion. J. Colloid Interface Sci. **274**, 118 (2004)
18. Y.D. Yin, G.Y. Hong, Morphology control of lanthanum hydroxide nanorods synthesized by hydrothermal microemulsion method. Chem. J. Chin. Univ. **26**(10), 1795 (2005)
19. Z.W. Song, J.F. Ma, X.Y. Li et al., Electrochemical synthesis and characterization of barium tungstate crystallites. J. Am. Ceram. Soc. **92**(6), 1 354 (2009)
20. Y. Wang, W. Mahler, Degenerate four-wave mixing of CdS/polymer composite. Opt. Commun. **61**, 233 (1987)
21. L.S. Cavalcante, J.C. Sczancoski, L.F. Lima et al., Synthesis, characterization, anisotropic growth and photoluminescence of $BaWO_4$. Cryst. Growth Des. **9**(2), 1002–1012 (2009)

Publisher's Note Springer Nature remains neutral with regard to jurisdictional claims in published maps and institutional affiliations.